Interaction of nephrocystin-4 and RPGRIP1 is disrupted by nephronophthisis or Leber congenital amaurosis-associated mutations

Ronald Roepman*†‡, Stef J. F. Letteboer*†, Heleen H. Arts*†, Sylvia E. C. van Beersum*†, Xinrong Lu§, Elmar Krieger¶, Paulo A. Ferreira§, and Frans P. M. Cremers*†

*Department of Human Genetics, Radboud University Nijmegen Medical Centre, P.O. Box 9101, 6500 HB, Nijmegen, The Netherlands; †Nijmegen Centre for Molecular Life Sciences, Nijmegen, The Netherlands; §Departments of Ophthalmology and Molecular Genetics and Microbiology, Duke University Medical Center, Erwin Road, Durham, NC 27710; and ¶Center for Molecular and Biomolecular Informatics, Radboud University Nijmegen, P.O. Box 9010, 6500 GL, Nijmegen, The Netherlands

Edited by Jeremy Nathans, The Johns Hopkins University School of Medicine, Baltimore, MD, and approved October 24, 2005 (received for review July 25, 2005)

RPGR-interacting protein 1 (RPGRIP1) is a key component of cone and rod photoreceptor cells, where it interacts with RPGR (retinitis pigmentosa GTPase regulator). Mutations in *RPGRIP1* lead to autosomal recessive congenital blindness [Leber congenital amaurosis (LCA)]. Most LCA-associated missense mutations in *RPGRIP1* are located in a segment that encodes two C2 domains. Based on the C2 domain of novel protein kinase Cε (PKCε), we built a 3D-homology model for the C-terminal C2 domain of RPGRIP1. This model revealed a potential Ca^{2+}-binding site that was predicted to be disrupted by a missense mutation in *RPGRIP1*, which was previously identified in an LCA patient. Through yeast two-hybrid screening of a retinal cDNA library, we found this C2 domain to specifically bind to nephrocystin-4, encoded by *NPHP4*. Mutations in *NPHP4* are associated with nephronophthisis and a combination of nephronophthisis and retinitis pigmentosa called Senior–Løken syndrome (SLSN). We show that RPGRIP1 and nephrocystin-4 interact strongly *in vitro* and *in vivo*, and that they colocalize in the retina, matching the panretinal localization pattern of specific RPGRIP1 isoforms. Their interaction is disrupted by either mutations in *RPGRIP1*, found in patients with LCA, or by mutations in *NPHP4*, found in patients with nephronophthisis or SLSN. Thus, we provide evidence for the involvement of this disrupted interaction in the retinal dystrophy of both SLSN and LCA patients.

retinal degeneration | RPGR protein complex | Senior–Løken | sensorineural disease

The X-linked gene *RPGR* (retinitis pigmentosa GTPase regulator) is mutated in patients with retinitis pigmentosa type 3 (RP3) (1, 2), cone or cone-rod dystrophy (COD1) (3, 4), atrophic macular degeneration (5), and RP in combination with impaired hearing and sinorespiratory infections (6). All RP3-associated missense mutations in *RPGR* have been identified in the N-terminal RCC1-homologous domain, and they disrupt the interaction with the C-terminal domain of RPGR-interacting protein 1 (RPGRIP1) (7, 8). Mutations in *RPGRIP1* lead to Leber congenital amaurosis (LCA), a genetically heterogeneous recessive disorder that is regarded to be the earliest and most severe form of all retinal dystrophies (9, 10). LCA accounts for at least 5% of all retinal dystrophies and is one of the main causes for blindness in children (11). RPGR and RPGRIP1 isoforms have been found to colocalize at the connecting cilia as well as the outer segments of rod and cone photoreceptors (12, 13). Differential localization among species has also been reported (12, 14), and different isoforms of RPGRIP1 have been described resulting from splicing variation (7, 14, 15). The distinct partitioning of a subset of RPGRIP1 isoforms between the nuclear and cytoplasmic compartments combined with the differential and limited proteolysis of RPGRIP1 among retinal neurons, and the impact of LCA-linked mutations in *RPGRIP1* in these processes, support the involvement of nucleocytoplasmatic signaling processes mediated by RPGRIP1 and its interacting partners in the pathogenesis of LCA, RP3, and allied diseases (15, 16). The presence of both RPGR and RPGRIP1 proteins in basal bodies and centrosomes of cultured dividing, but not interphase mammalian cells of nonretinal origin, suggests also a pleiotropic function of this protein complex (17). The absence of an RPGRIP1 isoform in *Rpgrip1*$^{-/-}$ mutant mice appears to lead to a defect in outer segment disk formation, suggesting a role in disk morphogenesis (18). *RPGRIP1* encodes three structurally different regions: an N-terminal coiled-coil domain, which possibly mediates homotypic and/or heterotypic interactions (13, 16); a C-terminal region that contains the RPGR-interacting domain (RID) (7); and a central region that contains a protein kinase C conserved region 2 (C2) motif (19). C2 domains are implicated in Ca^{2+}-dependent membrane docking of proteins and in mediating protein–protein interactions (20).

We analyzed the presumed scaffolding function of RPGRIP1 by identifying proteins that interact with its C2 domains, and identified nephrocystin-4 as an interactor toward a specific C2 domain of RPGRIP1 in the retina. This protein, which is also reported to exhibit a dynamic subcellular behavior (21), is associated with nephronophthisis type 4 (NPHP4), and a combination of nephronophthisis and retinitis pigmentosa, called Senior–Løken syndrome (SLSN) (22, 23). Our data show that LCA-associated mutations identified in *RPGRIP1*, or NPHP/SLSN-associated mutations identified in *NPHP4*, disrupt the RPGRIP1–nephrocystin-4 interaction, providing an explanation for the retinal component of SLSN.

Materials and Methods

DNA Constructs. Human retina Marathon-Ready cDNA (Clontech) was used to amplify the cDNA fragments of *NPHP4* and *RPGRIP1*. cDNA clones KIAA1005 and KIAA0673 were obtained from the Kazusa DNA Research Institute (24). Gateway-adapted constructs were created by using the Gateway cloning system (Invitrogen). Procedures to create constructs used for expression of different fragments of RPGRIP1, nephrocystin-4, and SYT1 are included in *Supporting Materials and Methods*, which is published as supporting information on the PNAS web site.

Conflict of interest statement: No conflicts declared.

This paper was submitted directly (Track II) to the PNAS office.

Abbreviations: LCA, Leber congenital amaurosis; RID, RPGR-interacting domain; RP, retinitis pigmentosa; SLSN, Senior–Løken syndrome.

‡To whom correspondence should be addressed. E-mail: r.roepman@antrg.umcn.nl.

Yeast Two-Hybrid Screening. A GAL4-based yeast two-hybrid system (HybriZAP, Stratagene) was used to identify proteins that interact with RPGRIP1$^{C2\text{-}C+C2\text{-}N}$, using methods described in ref. 25. Bovine RPGRIP1$^{C2\text{-}C+C2\text{-}N}$ was used as a bait to screen 1.2×10^6 clones of a bovine library of randomly primed retina cDNA (25).

Analysis of Interactions in Yeast. Positive prey clones were isolated and rescreened for transactivation of the reporter genes to rule out fortuitous interactions, as described in ref. 25. The interactions of the wild-type and mutated RPGRIP1 and nephrocystin-4 proteins were quantified by determining the β-galactosidase activity as reported in ref. 26.

Coimmunoprecipitation Assays. Epitope-tagged proteins for immunoprecipitation were expressed by using the following plasmids: pcDNA3-HA-N4$^{f\text{-}l}$/EXP (N-terminal HA-tag), pcDNA3-HA-N4-I/EXP (N-terminal HA-tag), p3xFLAG-RPGRIP1-b/EXP (N-terminal 3× FLAG-tag), p3xFLAG-RPGRIP1$^{C2\text{-}N+C2\text{-}C}$/EXP (N-terminal 3× FLAG-tag), and STRAD-FLAG and LKB1-myc control plasmids (27). Transfection of COS-1 cells, immunoprecipitation of the epitope-tagged proteins, and Western blot analysis are described in *Supporting Materials and Methods*.

GST Pull-Down. For the production of GST fusion proteins, BL21-DE3 cells were transformed with pDest-15/RPGRIP1$^{C2\text{-}C}$, pDest-15/RPGRIP1^{RID}, or pDest-15/N4-II expressing proteins fused to GST at their N terminus. GST fusion proteins were purified as described in ref. 26. The GST pull-down procedure is described in *Supporting Materials and Methods*.

Expression of Fluorescent Proteins. Fluorescent protein variants fused to N4$^{f\text{-}l}$ and RPGRIP1-b were expressed in COS-1 cells by using pDest-501 (N-terminal eCFP tag), pDest-504 (C-terminal eYFP tag), and pDest-733 (N-terminal mRFP tag). The cells were transfected and grown overnight on glass microscope slides, fixed, and analyzed by fluorescence microscopy as described in ref. 28.

Immunohistochemistry of Retinal Sections. Immunolocalization of the RPGRIP1 and nephrocystin-4 proteins in murine and bovine retinas was carried out essentially as shown in ref. 14, with minor variations. The affinity-purified antibodies MCW3 and MCW4 against the C2 domain of RPGRIP1 are described in refs. 12 and 15. The N4#5 and N4#6 antibodies were polyclonal mouse ascites, generated against human nephrocystin-4, KLH-conjugated peptide (C)NKRITYTNPYPSRR (Zymed Laboratories). The sections were coincubated with affinity-purified rabbit polyclonal MCW3 (5 μg/ml), MCW4 (3 μg/ml), Ab 39 (3 μg/ml), and N4#6 (1:100) for 1.5 h followed by three washes and a 1-h incubation with the secondary antibody (2.5 μg/ml). Then, sections were washed three times in 0.1% Triton X-100/1× PBS for 30 min, followed by three additional washes with 1× PBS for 10 min each. Visualization of retinal sections and localization of proteins were carried out as described in ref. 14.

Molecular Modeling and Identification of Potential Ca^{2+}-Binding Sites. The procedures used to build a 3D-homology model of RPGRIP1$^{C2\text{-}C}$ (amino acid residues 794–930) and to identify potential Ca^{2+}-binding sites in this domain are described in *Supporting Materials and Methods*.

Results

Homology Modeling Predicts Ca^{2+} Binding of RPGRIP1$^{C2\text{-}C}$. A conserved C2 domain signature was identified in RPGRIP1 and its orthologues (C2-C; Fig. 1*A* and Fig. 6, which is published as supporting information on the PNAS web site). Upstream of

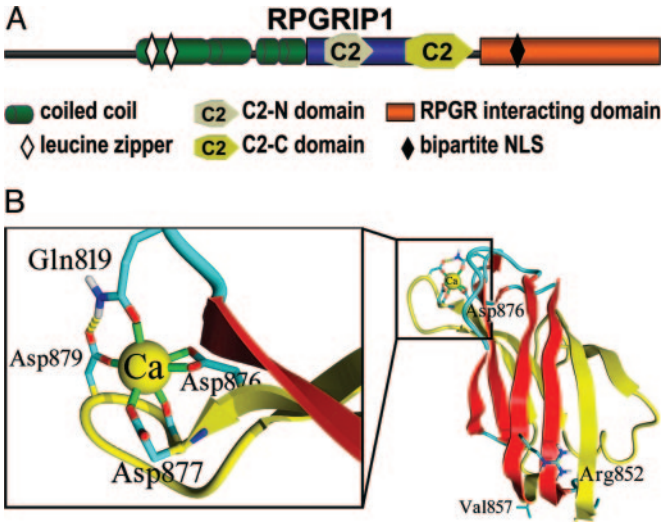

Fig. 1. Structure of RPGRIP1 and 3D-homology model of its C2-C domain. (*A*) Structure of human RPGRIP1 (GenBank NP_065099). (*B*) 3D-homology model of human RPGRIP1$^{C2\text{-}C}$ (*Right*), with the amino acid positions of residues that correspond to the mutations analyzed in this study. The part of the peptide chain colored yellow indicates the portion that is truncated in the RPGRIP1 p.V857fs mutant. (*B Left*) Close-up of the residues that are involved in the predicted Ca^{2+} binding.

RPGRIP1$^{C2\text{-}C}$, we identified a second, although truncated, C2 homologous domain (C2-N; Figs. 1*A* and 6). The C2 domains are encoded by exons 14–16, which are lacking in different splice variants of RPGRIP1 (7, 8). *RPGRIP1* mutations have been reported in patients with LCA (9) or CRD (29). As expected for these recessive conditions, the protein truncating mutations are evenly distributed along the gene. However, the missense mutations are clustered in the region containing the C2 domains, which points to a putative important role of this domain in retina function.

The closest homologue of RPGRIP1$^{C2\text{-}C}$ of known crystal structure was found to be the C2 domain of novel protein kinase Cε (PKCε) (30), which was therefore chosen as a template for building a homology model (Figs. 1*B* and 6). In the structural alignment, we identified a conserved residue (Asp-876) that, in classical Ca^{2+}-binding C2 domains, is an essential aspartate for Ca^{2+} binding. This enabled us to address the question as to whether RPGRIP1 can bind Ca^{2+}, given the potentially crucial role of Ca^{2+} for protein function. We added a Ca^{2+} ion to the homology model *in silico* and performed an energy minimization to optimize surrounding side chains. A putative Ca^{2+}-binding site with a high Ca^{2+} affinity could be identified involving the side chains of the conserved residues Asp-876, Asp-877, Asp-879, and Gln-819 (Fig. 1*B*).

Nephrocystin-4 Specifically Interacts with RPGRIP1$^{C2\text{-}C}$. To identify interactors for the C2 domains of RPGRIP1, we screened a randomly primed bovine yeast two-hybrid retina cDNA library (25), using RPGRIP1$^{C2\text{-}N+C2\text{-}C}$ as a bait. We initially isolated 27 independent prey clones, in which all four reporter genes were activated. Further analysis showed that only six of these clones bound to the C2-C domain. The clone that most strongly activated the reporter genes, C77, contained a fragment of nephrocystin-4 (assays 19–26 of Table 1, which is published as supporting information on the PNAS web site). This protein is encoded by *NPHP4*, the gene involved in nephronophthisis type 4 and SLSN (22, 23).

By assessment of the reporter gene activation in yeast, we found that the human counterpart of bovine nephrocystin-4

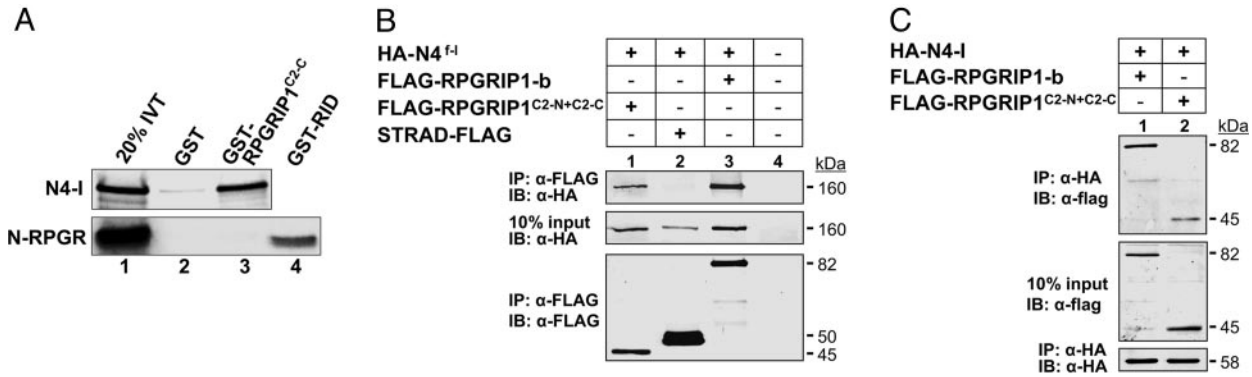

Fig. 2. RPGRIP1 interaction with nephrocystin-4. (*A*) GST-RPGRIP1$^{C2\text{-}C}$ efficiently pulled down *in vitro*-translated N4-I but not N-RPGR (lane 3). Unfused GST (lane 2) pulled down neither, whereas, as a control, GST-RPGRIP1^{RID} pulled down N-RPGR (lane 4). Lane 1 shows 20% of the *in vitro*-translated protein input (20% IVT). (*B* and *C*) Immunoprecipitation (IP) of nephrocystin-4 and RPGRIP1. (*B*) The immunoblot (IB) in *Top* shows that HA-nephrocystin-4$^{f\text{-}I}$ (160 kDa, input shown in *Middle*) coimmunoprecipitated with FLAG-RPGRIP1$^{C2\text{-}N+C2\text{-}C}$ (lane 1) and with FLAG-RPGRIP1-b (lane 3), but not with STRAD-FLAG (lane 2) or mock-transfected cell lysate (lane 4). The anti-FLAG immunoprecipitates are shown in *Bottom*. (*C*) FLAG-RPGRIP1$^{C2\text{-}N+C2\text{-}C}$ (lane 1) and FLAG-RPGRIP1-b (lane 2) coimmunoprecipitated with the HA-tagged nephrocystin-4-I fragment (HA-N4-I, 58 kDa). Protein inputs are shown in *Middle*; anti-HA immunoprecipitates are shown in *Bottom*.

fragment, nephrocystin-4-I (Fig. 7, which is published as supporting information on the PNAS web site), interacts with RPGRIP1$^{C2\text{-}N+C2\text{-}C}$, as well as with RPGRIP1$^{C2\text{-}C}$ (Table 1, assays 27–29 and 38) and its homologue KIAA1005$^{C2\text{-}C}$ that is 52% identical (Table 1, assays 47 and 48), but not with the prototype C2 domain of synaptotagmin 1, SYT1^{C2}, which is 20% identical (Table 1, assays 49 and 50). Furthermore, we could pinpoint the RPGRIP1-interacting domain of nephrocystin-4 to amino acids 591–960 of GenBank entry NP_055917, encoded by exons 15–21 of *NPHP4* (Table 1, assays 29–46, and Fig. 7).

We tested whether interaction between RPGRIP1 and nephrocystin-4 was direct by carrying out *in vitro* GST pull-down assays. We found that GST-RPGRIP1$^{C2\text{-}C}$ efficiently pulled down N4-I but not N-RPGR (Fig. 2*A*, lane 3), which was pulled down by the RID (GST-RPGRIP1^{RID}; Fig. 2*A*, lane 4). Reciprocal GST pull-down assays from COS-1 cell lysates confirmed these findings (Fig. 8, which is published as supporting information on the PNAS web site). Analysis of this *in vitro* interaction in presence of the Ca^{2+} chelators EDTA and EGTA indicates that the binding is Ca^{2+}-independent (results not shown).

To complement these results in a cell-based assay, epitope-tagged full-length nephrocystin-4 (N4$^{f\text{-}I}$) and RPGRIP1-b, which also contains the RID (7, 8), were expressed in COS-1 cells. We performed immunoprecipitation assays using anti-FLAG antibodies and were able to show that HA-N4$^{f\text{-}I}$ efficiently coimmunoprecipitated with FLAG-RPGRIP1, both with the C2-N + C2-C domain (Fig. 2*B*, lane 1) and with full-length RPGRIP1-b (Fig. 2*B*, lane 3), but not with the unrelated protein STRAD (Fig. 2*B*, lane 2). Furthermore, immunoprecipitation experiments with anti-HA antibodies showed that both RPGRIP1 proteins also coimmunoprecipitated with HA-N4-I (Fig. 2*C*, lanes 1 and 2). The reciprocal assays of these experiments confirmed these results (Fig. 9, which is published as supporting information on the PNAS web site).

Using different fluorescent protein epitope tags (eCFP and eYFP) in fluorescence microscopy, we could show that in COS-1 cells expressing only the full-length nephrocystin-4 fused to eCFP, the protein was localized in specific structures around, but not in, the nucleus (Fig. 3*B*). Interestingly, in cells only transfected with RPGRIP1-b-eYFP, the protein was localized in the nucleus (Fig. 3*C*), suggesting that the bipartite nuclear localization motif in the RID of RPGRIP1 (bipartite NLS, Fig. 1*A*) may underlie the translocation to the nucleus. Coexpression of

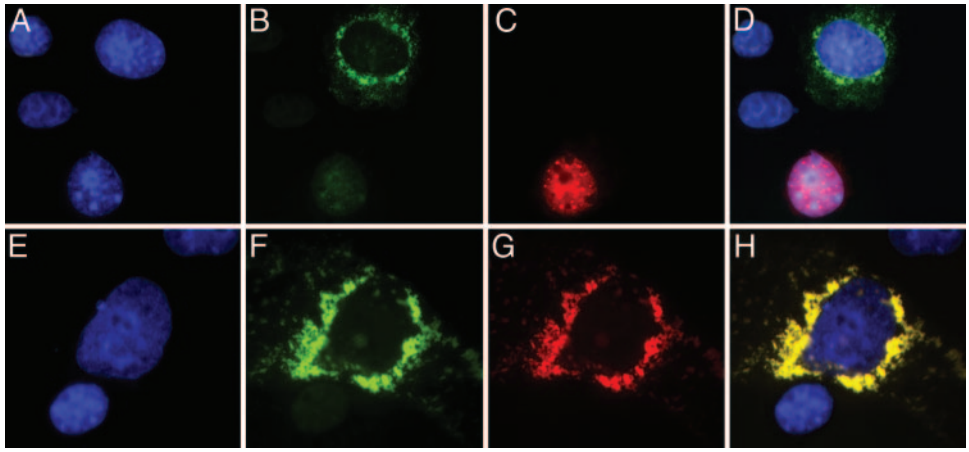

Fig. 3. Nephrocystin-4 colocalizes with RPGRIP1 upon overexpression in COS-1 cells. (*A* and *E*) DAPI staining of the cell nuclei (blue signal). (*B*) eCFP-nephrocystin-4 (green signal) localized in the cytoplasm around, but not in, the cell nucleus (top cell) when singly transfected. (*C*) eYFP-RPGRIP1 (red signal) localized only in the nucleus (bottom cell) when singly transfected. (*D*) overlay of *A–C*. (*F–H*) When both proteins are expressed in the same cell (*F*, eCFP-nephrocystin-4; *G*, eYFP-RPGRIP1), they colocalize in the cytoplasm (*H*, overlay of *E–G*, yellow signal).

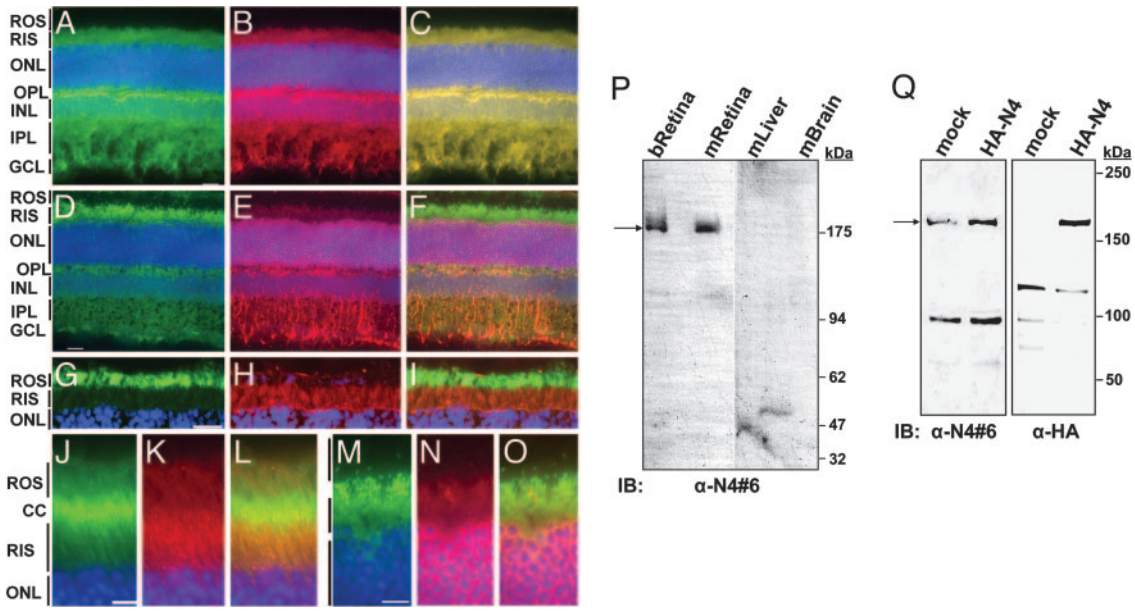

Fig. 4. Immunolocalization of nephrocystin-4 and RPGRIP1 proteins in the retina and Western blot analysis of nephrocystin-4. (*A–O*) Localization of nephrocystin-4 and RPGRIP1 proteins in the retina. Focal-plane images of radial retinal cryosections shown in *A–C* are, respectively, murine retinal sections immunostained with MCW3 Ab against the C2 domain of RPGRIP1, Ab#6 against nephrocystin-4, and an overlay of *A* and *B*. The C2-containing RPGRIP1 isoform(s) colocalized perfectly with nephrocystin-4 throughout the retina. *D–F* are, respectively, murine retinal sections immunostained with Ab39 against the RID domain of RPGRIP1, N4#6 against nephrocystin-4, and an overlay of *D* and *E*. *G–I* are, respectively, the photoreceptor layer of a bovine retinal section immunostained with MCW4 Ab against the C2 domain of RPGRIP1, Ab#6 against nephrocystin-4, and an overlay of *G* and *H*. *J–L*, are respectively, the photoreceptors layer of a murine retinal section immunostained with MCW4 Ab against the C2 domain of RPGRIP1, Ab#6 against nephrocystin-4, and an overlay of *J* and *K*. *M–O* are, respectively, the photoreceptors layer of a murine retinal section immunostained with Ab39 against the RID domain of RPGRIP1, Ab#6 against nephrocystin-4, and an overlay of *M* and *N*. (Scale bars: *J* and *M*, 10 μm; *A* and *D*, 50 μm.) ROS, rod outer segments; RIS, rod inner segments; ONL, outer nuclear layer; OPL, outer plexiform layer; INL, inner nuclear layer; IPL, inner plexiform layer; GCL, ganglion cell layer; CC, connecting cilium. (*P*) Immunoblot of tissue homogenates from mouse and bovine, showing that anti-nephrocystin-4 antibody N4#6 specifically detects a single protein (indicated by an arrow) in the retinal extracts of mouse and bovine. (*Q*) Recombinant HA-nephrocystin-4 was detected by antibody N4#6 (second lane) as well as by anti-HA (fourth lane) on immunoblots of COS-1 cell lysates. In lysates from mock-transfected cells, only the N4#6 antibody detects a specific signal of lower intensity but of exactly the same size (indicated by an arrow).

nephrocystin-4 with RPGRIP1 fully retained the latter to the cytoplasm, because no nuclear signal could be detected in these cells (Fig. 3 *E–H*), and resulted *in vivo* in the colocalization of both proteins. Exchanging the eYFP tag with mRFP or switching the fluorescent protein tags between RPGRIP1 and nephrocystin-4 did not influence these (co)localization results (Fig. 10, which is published as supporting information on the PNAS web site).

RPGRIP1 and Nephrocystin-4 Colocalize in the Retina. Nephrocystin-4 exhibited panretinal expression with two independently raised antibodies, N4#5 and N4#6. The antibodies prominently stained the branching processes emanating from inner nuclear neurons, the postsynaptic layer of the outer plexiform layer, and the cell bodies of photoreceptors (Fig. 4 *B* and *E*). The staining toward nephrocystin-4 was highly specific because its was fully blocked by preincubation of the primary antibodies with the cognate peptide epitope, and preimmune serum gave no signal (data not shown). Nephrocystin-4 was also diffusely localized throughout the inner segment compartment of photoreceptors (Fig. 4 *B* and *E*) and colocalized perfectly with C2-containing RPGRIP1 isoforms (Fig. 4 *A–C*) and partially with an antibody against the RID of RPGRIP1 (Fig. 4 *B* and *D–F*). The outer segments of murine (Fig. 4 *B*, *E*, *K*, and *N*) and bovine (Fig. 4*H*) retinas lacked any nephrocystin-4 staining. In specific focal planes, we observed only a very limited overlap of localization between RPGRIP1 and nephrocystin-4 in the connecting cilium of photoreceptors (Fig. 4 *J–O*). Specificity of the N4#6 antibody was confirmed on immunoblots (Fig. 4 *P* and *Q*). A single protein with an apparent molecular mass of ≈180 kDa was detected in the retina of bovine and mouse but not in the liver and brain (Fig. 4*P*). Furthermore, in COS-1 cell lysates, the antibody detects the HA-tagged recombinant full-length nephrocystin-4 protein (HA-N4$^{f\text{-}l}$), which is also detected by the anti-HA antibody (Fig. 4*Q*). In mock-transfected cells, the endogenous full-length nephrocystin-4 protein and a smaller isoform of ≈97 kDa were detected (Fig. 4*Q*). These features further confirm the specificity of the nephrocystin-4 antibody used.

RPGRIP1 and NPHP4 Mutations Disrupt Their Interaction. Four of 6 LCA-associated amino acid substitutions in RPGRIP1 (9, 31) and 10 of 19 NPHP/SLSN-associated amino acid substitutions in nephrocystin-4 (32) are located in or very near to the interacting domains of both proteins (Fig. 5 *A* and *C*). We have introduced a subset of these variants, as well as protein truncating mutations, into both bait and prey plasmids encoding these domains and analyzed the effects on the interaction of RPGRIP1 with nephrocystin-4 using the yeast two-hybrid system (Fig. 5 *B* and *D* and Table 2, which is published as supporting information on the PNAS web site) and by coimmunoprecipitation (Fig. 5*E*). The RPGRIP1 p.D876G and p.R890X alterations (Fig. 5 *B* and *E* and Table 2, assays 12 and 13) and the p.G746E and p.V857fs alterations (Table 2, assays 9 and 11) severely disrupted the interaction with nephrocystin-4, consistent with the pathologic character of these variants. We also introduced the p.R852Q variant that was found heterozygously in an isolated LCA patient (R.R. and F.P.M.C., unpublished data). This amino acid exchange did not affect the interaction (Fig. 5 *B* and *E* and Table 2, assay 10), which could indicate that this variant is nonpathologic. This finding matched with the homology model (Fig. 1*B*),

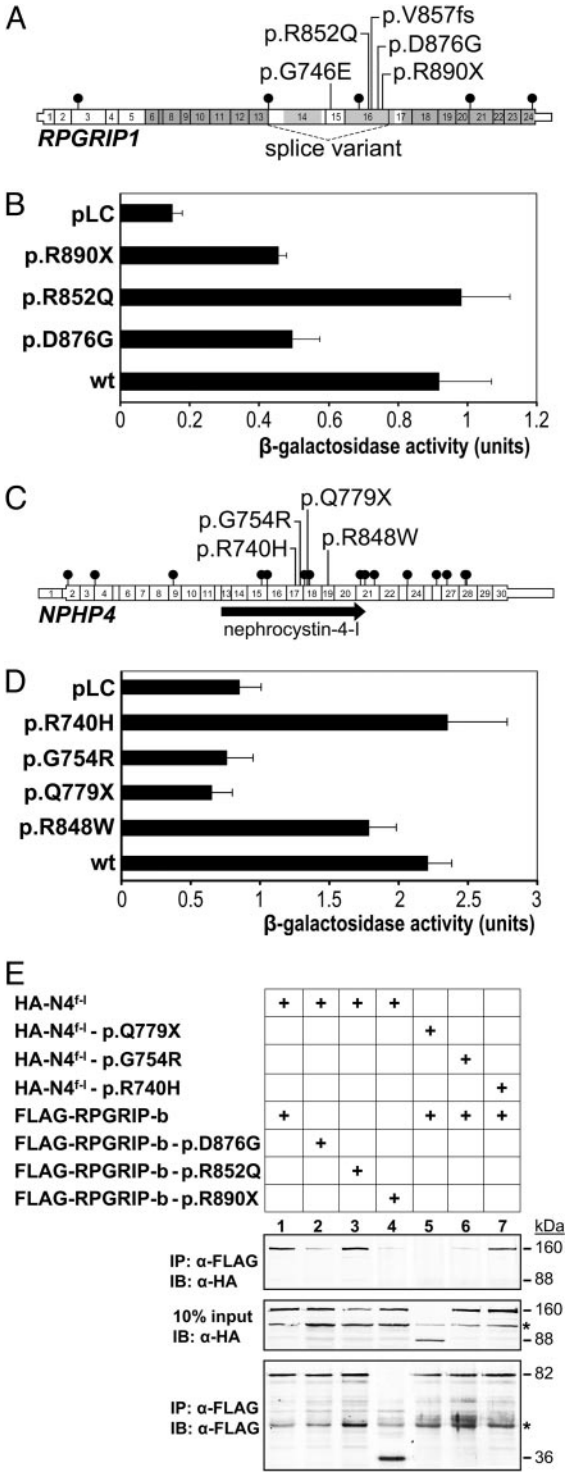

Fig. 5. *RPGRIP1* and *NPHP4* mutations disrupt the interaction of nephrocystin-4 with RPGRIP1. (*A*) Exon structure of *RPGRIP1* and mutations identified in this gene. The sequence variants that were analyzed in the yeast two-hybrid system in this study are annotated; the other missense mutations that have been reported (9, 29, 31) are indicated by filled circles. (*B*) Wild-type and mutated human RPGRIP1$^{C2\text{-}C}$ proteins (fused to GAL4-AD) were assessed for interaction with nephrocystin-4-I, fused to the GAL4-BD domain. An ONPG assay was used to quantify the β-galactosidase activity of the yeast cells (in arbitrary units), which is indicated by the black bars. pBD-LaminC/pAD-pSV40 (pLC) was used as a negative control, indicating the somewhat leaky activation of this reporter gene without selection for transactivation. (*C*) Exon structure of *NPHP4* and mutations identified in this gene. The sequence variants that were analyzed in the yeast two-hybrid system in this study are annotated; the other missense mutations that have been reported (32) are indicated by filled circles. (*D*) Wild-type and mutated human nephrocystin-4-I proteins (N4, fused to GAL4-BD) were assessed for interaction with RPGRIP1$^{C2\text{-}C}$, fused to the GAL4-AD domain. (*E*) Immunoprecipitation (IP) of wild-type and mutated HA-nephrocystin-4$^{f\text{-}I}$ and FLAG-RPGRIP1-b. Coimmunoprecipitation is shown in *Top*, protein inputs are shown in *Middle*, and anti-FLAG immunoprecipitates are shown in *Bottom*. The sizes (in kDa) of the proteins corresponding with the specific antibody signals are indicated. Cross-reacting signals, present in all samples, are marked with an asterisk.

in which the p.R852Q exchange is predicted to be of little structural consequence, because it is on the opposite side from Arg-50 in the structural homologue (30), which is essential in membrane binding. When membrane binding is involved, it would face away from the membrane. Because the residue is also not conserved among species, this variant is unlikely to be pathologic.

Introduction of the p.G754R exchange, reported to be associated with nephronophthisis (23), and the SLSN-associated p.Q779X mutation (22) fully disrupted the interaction of nephrocystin-4 with RPGRIP1 (Fig. 5 *D* and *E*). In contrast, the p.R740H and p.R848W amino acid substitutions that were reported to be nonpathologic (22, 23) showed no significant effect on the interaction.

Discussion

The data reported herein and elsewhere support that RPGRIP1 isoforms mediate multiple biological processes that are vital for retinal function (7, 14–16). This variety of functions likely reflects the molecular diversity of RPGRIP1 isoforms and composition of the RPGRIP1 interactome. We show that the C2 domain of RPGRIP1, encoded by a splice variant of *RPGRIP1*, strongly interacts with nephrocystin-4 and that human mutations in these abrogate the interaction. Mutations in the gene encoding nephrocystin-4 (*NPHP4*) are associated with nephronophthisis type 4 (NPHP4) and SLSN (22, 23). Nephronophthisis is the most frequent monogenic cause for end-stage renal failure in children and young adults (33, 34), who suffer from interstitial inflammation, renal fibrosis, and cyst formation at the corticomedullary border (33). SLSN is characterized by nephronophthisis in combination with retinal degeneration of variable severity (35, 36). Here, we have shown that missense and nonsense mutations in *RPGRIP1* (in LCA patients) or *NPHP4* (in nephronophthisis and SLSN patients) disrupt the interaction between RPGRIP1 and nephrocystin-4, whereas nonpathologic variants do not. This finding might, at least partially, explain the retinal degeneration of the SLSN syndrome, as well as LCA patients. Because no kidney phenotype has been reported in LCA patients with *RPGRIP1* mutations, it is unlikely that a disrupted RPGRIP1–nephrocystin-4 interaction also primarily leads to nephronophthisis. Our yeast two-hybrid data also support an interaction of nephrocystin-4 with the C2 domain of the only RPGRIP1 homologue, KIAA1005. In light of *KIAA1005*'s greater abundance in the kidney than RPGRIP1, and because mutations in *NPHP4* also affect the nephrocysin-4–RPGRIP1 interaction (results not shown), it is possible that compensatory mechanisms between RPGRIP1 and KIAA1005 (and/or other RPGRIP1 partners) play a role in the expressivity of ocular-renal diseases phenotypes.

Nephrocystin-4 has recently been found to be abundantly present at the subcortical plasma membrane region of polarized renal epithelial cells, in the centrosomes of dividing cells, and, to a lesser extent, in the primary cilia of highly confluent cell cultures (21), thus mirroring the dynamic properties of RPGRIP1. The shared subcellular properties of RPGRIP1 and nephrocystin-4 are further strengthened by the panretinal colocalization of nephrocystin-4 and RPGRIP1 isoforms containing

the C2 domain. The interaction of nephrocystin-4 with RPGRIP1 identified here strongly suggests an important functional link of these proteins in the disease pathogenesis of RP/LCA and NPHP/SLSN.

By combining 3D-homology modeling of the C2-C domain with the RPGRIP1–nephrocystin-4 interaction data, we were able to assess the pathogenicity of the identified alterations. One interesting RPGRIP1 alteration that was strongly suggested to be pathologic, p.D876G, disrupted the putative Ca^{2+}-binding site of the C2-C domain and fully disrupted the interaction with nephrocystin-4. However, the interaction of the wild-type proteins was not affected by Ca^{2+} chelators, indicating that this protein–protein interaction is Ca^{2+}-independent. Therefore, if Ca^{2+} does bind to this protein, this C2 domain may have evolved to provide multiple functions, e.g., additionally binding phospholipids in a Ca^{2+}-dependent manner similar to synaptotagmin (37).

Important remaining questions concern the observed wide variation of clinical phenotypes in patients with *NPHP4* mutations, and the fact that the *NPHP4* mutation p.G754R, which disrupts the interaction between nephrocystin-4 and RPGRIP1, is found in a patient with nephronophthisis without signs of RP. Because expression of RP is progressive and often variable in severity, it is possible that the nephronophthisis patient might still develop RP at a later stage. It is also possible that additional factors in the retinal complex need to be disrupted to result in a Senior–Løken phenotype. The fact that the mutation in the Senior–Løken patient results in a truncation of the protein seems to support this hypothesis. Because nephrocystin-4 has been reported to bind to nephrocystin-1 at its N-terminal region (22), and our preliminary data indicate that additional proteins bind to the different domains of RPGRIP1 (R.R. and P.A.F., unpublished data), this protein might act as a scaffold for recruitment of multiple partners that determine the subcellular properties of this dynamic multiassembly complex. One or more of these partners might compensate for loss of activity of one of the other complex members, which would then suppress a retinal phenotype. This hypothesis combined with the fact that all patients with mutations in the recently identified *IQCB1* (*NPHP5*) gene develop a retinal phenotype, and that the encoded nephrocystin-5 protein may exist in a complex with RPGR (38), builds evidence for an emerging retinal protein complex with a pleiotropic and dynamic behavior in retina and kidney (patho)physiology.

We thank H. G. Brunner for helpful discussions on the work; A. F. Baas for providing the LKB1 and STRAD constructs; D. Esposito for providing the pDest-501, pDest-504, and pDest-733 vectors; and P. Duijf for providing the pcDNA3-HA/DEST vector. This work was supported by British Retinitis Pigmentosa Society Grant GR257 (to F.P.M.C.), European Commission IP "EVI-GenoRet" LSHG-CT-2005-512036 (to R.R. and F.P.M.C.), and National Institutes of Health Grants EY11993 and EY012665 (to P.A.F.). P.A.F. is the Jules and Doris Stein Research to Prevent Blindness Professor.

1. Roepman, R., van Duynhoven, G., Rosenberg, T., Pinckers, A. J. L. G., Bleeker-Wagemakers, E. M., Bergen, A. A. B., Post, J., Beck, A., Reinhardt, R., Ropers, H.-H., *et al.* (1996) *Hum. Mol. Genet.* **5,** 1035–1041.
2. Meindl, A., Dry, K., Herrmann, K., Manson, F., Ciccodicola, A., Edgar, A., Carvalho, M. R., Achatz, H., Hellebrand, H., Lennon, A., *et al.* (1996) *Nat. Genet.* **13,** 35–42.
3. Demirci, F. Y., Rigatti, B. W., Wen, G., Radak, A. L., Mah, T. S., Baic, C. L., Traboulsi, E. I., Alitalo, T., Ramser, J. & Gorin, M. B. (2002) *Am. J. Hum. Genet.* **70,** 1049–1053.
4. Yang, Z., Peachey, N. S., Moshfeghi, D. M., Thirumalaichary, S., Chorich, L., Shugart, Y. Y., Fan, K. & Zhang, K. (2002) *Hum. Mol. Genet.* **11,** 605–611.
5. Ayyagari, R., Demirci, F., Liu, J., Bingham, E., Stringham, H., Kakuk, L., Boehnke, M., Gorin, M., Richards, J. & Sieving, P. (2002) *Genomics* **80,** 166–171.
6. Zito, I., Downes, S. M., Patel, R. J., Cheetham, M. E., Ebenezer, N. D., Jenkins, S. A., Bhattacharya, S. S., Webster, A. R., Holder, G. E., Bird, A. C., *et al.* (2003) *J. Med. Genet.* **40,** 609–615.
7. Roepman, R., Bernoud-Hubac, N., Schick, D. E., Maugeri, A., Berger, W., Ropers, H. H., Cremers, F. P. M. & Ferreira, P. A. (2000) *Hum. Mol. Genet.* **9,** 2095–2105.
8. Boylan, J. P. & Wright, A. F. (2000) *Hum. Mol. Genet.* **9,** 2085–2093.
9. Dryja, T. P., Adams, S. M., Grimsby, J. L., McGee, T. L., Hong, D. H., Li, T., Andreasson, S. & Berson, E. L. (2001) *Am. J. Hum. Genet.* **68,** 1295–1298.
10. Hanein, S., Perrault, I., Gerber, S., Tanguy, G., Barbet, F., Ducroq, D., Calvas, P., Dollfus, H., Hamel, C., Lopponen, T., *et al.* (2004) *Hum. Mutat.* **23,** 306–317.
11. Cremers, F. P. M., van den Hurk, J. A. J. M. & den Hollander, A. I. (2002) *Hum. Mol. Genet.* **11,** 1169–1176.
12. Mavlyutov, T. A., Zhao, H. & Ferreira, P. A. (2002) *Hum. Mol. Genet.* **11,** 1899–1907.
13. Hong, D. H., Yue, G., Adamian, M. & Li, T. (2001) *J. Biol. Chem.* **276,** 12091–12099.
14. Lu, X. & Ferreira, P. A. (2005) *Invest. Ophthalmol. Vis. Sci.* **46,** 1882–1890.
15. Castagnet, P., Mavlyutov, T., Cai, Y., Zhong, F. & Ferreira, P. (2003) *Hum. Mol. Genet.* **12,** 1847–1863.
16. Lu, X., Guruju, M., Oswald, J. & Ferreira, P. A. (2005) *Hum. Mol. Genet.* **14,** 1327–1340.
17. Shu, X., Fry, A. M., Tulloch, B., Manson, F. D., Crabb, J. W., Khanna, H., Faragher, A. J., Lennon, A., He, S., Trojan, P., *et al.* (2005) *Hum. Mol. Genet.* **14,** 1183–1197.
18. Zhao, Y., Hong, D. H., Pawlyk, B., Yue, G., Adamian, M., Grynberg, M., Godzik, A. & Li, T. (2003) *Proc. Natl. Acad. Sci. USA* **100,** 3965–3970.
19. Rizo, J. & Südhof, T. C. (1998) *J. Biol. Chem.* **273,** 15879–15882.
20. Nalefski, E. A. & Falke, J. J. (1996) *Protein Sci.* **5,** 2375–2390.
21. Mollet, G., Silbermann, F., Delous, M., Salomon, R., Antignac, C. & Saunier, S. (2005) *Hum. Mol. Genet.* **14,** 645–656.
22. Mollet, G., Salomon, R., Gribouval, O., Silbermann, F., Bacq, D., Landthaler, G., Milford, D., Nayir, A., Rizzoni, G., Antignac, C., *et al.* (2002) *Nat. Genet.* **32,** 300–305.
23. Otto, E., Hoefele, J., Ruf, R., Mueller, A. M., Hiller, K. S., Wolf, M. T., Schuermann, M. J., Becker, A., Birkenhager, R., Sudbrak, R., *et al.* (2002) *Am. J. Hum. Genet.* **71,** 1161–1167.
24. Suyama, M., Nagase, T. & Ohara, O. (1999) *Nucleic Acids Res.* **27,** 338–339.
25. Roepman, R., Schick, D. & Ferreira, P. A. (2000) *Methods Enzymol.* **316,** 688–704.
26. Kantardzhieva, A., Gosens, I., Alexeeva, S., Punte, I. M., Versteeg, I., Krieger, E., Neefjes-Mol, C. A., den Hollander, A. I., Letteboer, S. J., Klooster, J., *et al.* (2005) *Invest. Ophthalmol. Vis. Sci.* **46,** 2192–2201.
27. Baas, A. F., Boudeau, J., Sapkota, G. P., Smit, L., Medema, R., Morrice, N. A., Alessi, D. R. & Clevers, H. C. (2003) *EMBO J.* **22,** 3062–3072.
28. Weterman, M. A., van Groningen, J. J., Tertoolen, L. & van Kessel, A. G. (2001) *Proc. Natl. Acad. Sci. USA* **98,** 13808–13813.
29. Hameed, A., Abid, A., Aziz, A., Ismail, M., Mehdi, S. Q. & Khaliq, S. (2003) *J. Med. Genet.* **40,** 616–619.
30. Ochoa, W. F., Garcia-Garcia, J., Fita, I., Corbalan-Garcia, S., Verdaguer, N. & Gomez-Fernandez, J. C. (2001) *J. Mol. Biol.* **311,** 837–849.
31. Gerber, S., Perrault, I., Hanein, S., Barbet, F., Ducroq, D., Ghazi, I., Martin-Coignard, D., Leowski, C., Homfray, T., Dufier, J. L., *et al.* (2001) *Eur. J. Hum. Genet.* **9,** 561–571.
32. Hoefele, J., Sudbrak, R., Reinhardt, R., Lehrack, S., Hennig, S., Imm, A., Muerb, U., Utsch, B., Attanasio, M., O'Toole, J. F., *et al.* (2005) *Hum. Mutat.* **25,** 411.
33. Fanconi, G., Hanhart, E. & Albertini, A. (1951) *Hel. Pediatr. Acta* **6,** 1–49.
34. Saunier, S., Salomon, R. & Antignac, C. (2005) *Curr. Opin. Genet. Dev.* **15,** 324–331.
35. Senior, B., Friedmann, A. I. & Braudo, J. L. (1961) *Am. J. Ophthalmol.* **52,** 625–633.
36. Løken, A. C., Hanssen, O., Halvorsen, S. & Jølster, N. J. (1961) *Acta Paediatr.* **50,** 177–184.
37. Rickman, C. & Davletov, B. (2003) *J. Biol. Chem.* **278,** 5501–5504.
38. Otto, E. A., Loeys, B., Khanna, H., Hellemans, J., Sudbrak, R., Fan, S., Muerb, U., O'Toole, J. F., Helou, J., Attanasio, M., *et al.* (2005) *Nat. Genet.* **37,** 282–288.